

A WIDE-BAND SPACEBORNE SPECTROGRAPH FOR MONITORING OF THE EARTH'S ATMOSPHERE

A.A. Cheremisin, V.I. Nalivaiko, L.V. Granitskii, S.F. Zagrabchuk, P.A. Chubakov, S.A. Veselkov, and V.V. Slabko

*Scientific-Research Physical-Technical Institute at the Krasnoyarsk State University
Krasnoyarsk State Technical University
Institute of Automation and Electrical Measurement,
Siberian Branch of the Russian Academy of Sciences, Novosibirsk
Received December 3, 1997*

A prototype of a small-size wide-band rapid spectrograph for an integrated study and monitoring of the atmospheric state from onboard artificial satellites is described and results of its laboratory testing are presented. The spectrograph comprises concave diffraction holography gratings with curvilinear slits, variable spacing, and flat focusing field, whose recording conditions are determined starting from an optimal arrangement of optical parts and aberration minimization. This spectrograph is capable of simultaneous recording of the radiation spectrum between 160–700 nm with a spectral resolution of ≤ 1 nm and a spatial resolution of 1 min of arc with the help of photodiode strips.

The current state of the art in the development of satellite systems for studying and monitoring of the atmospheric state allows for monitoring of the environmental pollution which brings the threat of an ecological disaster. Satellite measurements provide the means for obtaining global information about the atmospheric state and the content of many atmospheric constituents with sufficient data sampling rate and satisfactory accuracy.^{1–3}

A problem of detection of short-time local environmental effects of anthropogenic or natural origin is of special interest. These environmental effects happen, for example, when rockets are launched, chemical substances and plasma are injected into (or exploded in) the atmosphere, upon exposure to intense UV and radiowave radiation sources, during volcanic eruptions, industrial emissions, etc.

An integrated character of remote sensing problem calls for specific requirements to the parameters of satellite instrumentation, in particular, the necessity of measuring in a wider spectral range to retrieve simultaneously a number of the atmospheric parameters. It should be noted that recent trends in the development of satellite methods are to extend the list of measurable minor atmospheric gaseous constituents, to increase measurement accuracy and sensing range, to improve spatiotemporal resolution, and to estimate the integral physical state of the atmosphere.¹

To solve the problems of laser sensing, unique satellite instrumentation should be developed.^{4–6} Optimal experimental design with the use of satellite systems incorporates informational, engineering, and commercial aspects. In particular, the cost of experiments, the mass and overall dimensions of the

instrumentation, the energy consumption, and the amount of information stored onboard and transmitted to ground-based stations should be minimized.⁷

Degradation of optical systems under the effect of space also should be compensated.⁸

The spectral method is one of the main and most informative methods of remote sensing of the atmosphere. A great variety of spectrometer schemes were used in practice of space research of the atmosphere in the visible and UV ranges. The spectrometers built around dual-beam monochromators with superposition of dispersed constituents were used in the near-UV range^{9,10}; for example, the BUVS-1 apparatus operated in the wavelength range¹⁰ between 280–340 nm with the resolution $\Delta\lambda = 1$ nm. Its field-of-view angle was 16°. The Vodsvort scheme in combination with special mechanical grating collimators^{11–13} was used in the spectrometers operating in the far-UV range.

To provide a wide spectral range of measurements, the Spacelab-1 apparatus was equipped with a set of five simultaneously operating spectrometers¹¹; four of them were almost identical in design and covered the wavelength range from $\lambda = 120$ to 1200 nm, $\Delta\lambda = 15$ nm. The fifth spectrometer operated in the range 30–120 nm, $\Delta\lambda = 10$ nm. Its field-of-view angle was 0.65°. The wide wavelength range of the spectrometer described in Ref. 13 (85–395 nm, $\Delta\lambda = 0.4$ –1.2 nm) was achieved by means of splitting the spectrum into three spectral channels with the use of the second and third diffraction orders, three entrance slits, and three radiation detectors. Its field-of-view was $0.14 \times 3.8^\circ$. The Ebert-Fasty scheme⁴ was most widespread. This scheme was used in the design

of two monochromators of the BUV and SBUV/(TOMS) apparatuses.¹⁴ The largest set of satellite data on the global ozone distribution was obtained with the BUV and SBUV/(TOMS) apparatuses. The SBUV apparatus operates in the wavelength range $\lambda = 160\text{--}400$ nm, $\Delta\lambda = 1$ nm; its field-of-view is $12\times 12^\circ$, its aperture ratio is F:5. The apparatuses that explored Mars and Venus were designed in the Ebert-Fasty scheme¹⁵ and more compact autocollimation scheme.¹⁶ All these apparatuses allowed for spectral scanning by rotation of these or those optical parts. In this case, nonsimultaneous measurements at all wavelengths may cause the distortion of the spectrum due to fast orbiting of a space vehicle and spatiotemporal variations of the atmospheric parameters.

In the latter half of the 80s a trend was evident toward the use of spectrographs and Rowland schemes.⁴ This was because of the advent of new hardware including high-sensitive linear and matrix photodetectors, microprocessors for image interpretation, and new image intensifiers, for example, microchannel plates and holographic diffraction gratings. The holographic gratings have some advantages over mechanical ones, namely, they allow one to eliminate or, more exactly, to reduce significantly several types of aberrations. This makes it possible to develop rapid devices designed in the Rowland scheme and to suppress significantly the diffraction orders higher than the first one.

By the end of the 80s the holographic gratings were computed for the far-UV and soft X-ray ranges.¹⁷ A spectrometer intended to explore the

Halley comet that comprised all the above enumerated units was described in Ref. 4. To extend the wavelength range to include 120–1800 nm, the initial beam was split into three beams. Three spectral channels were designed as stand-alone units, namely, the UV channel between 1200–2900 Å, $\Delta\lambda = 10$ Å, the visible channel between 2800–7100 Å, $\Delta\lambda = 25$ Å, and the near-IR channel between 0.8–1.8 μm, $\lambda/\Delta\lambda = 70$.

The Scientific-Research Physical-Technical Institute at the Krasnoyarsk State University in collaboration with the Institute of Automation and Electrical Measurement, SB RAS with the participation of the Krasnoyarsk State University has been developing a small-size airborne wide-band high-sensitive spectrometer since 1988. It comprises holographic diffraction gratings and is capable of simultaneous recording the wavelength spectrum between 160–700 nm with a spectral resolution of about 1 nm and a spatial resolution of about 1 min of arc. The spectrometer is intended for an integrated study and monitoring of the atmospheric state from a board of an artificial Earth's satellite. As a result, a prototype has been developed and tested under laboratory conditions.

To produce the gratings, a new inorganic photoresist – chalcogenide glass – was evaporated in vacuum onto concave substrates made from pyroceramics. This vaporized glass coating of the photoresist ensures high optical quality of its surface and low level of background scattering by these gratings, and the pyroceramic substrates with low expansion ratios can operate under severe conditions.

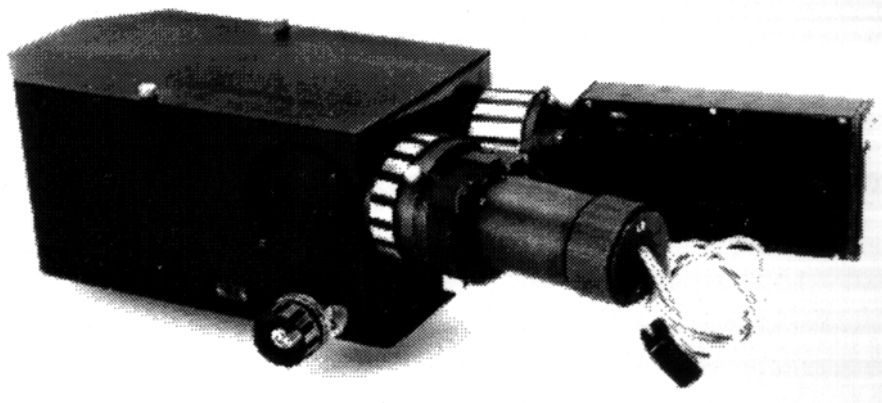


FIG. 1. External view of the single-band small-size spectrograph with a changeable source of radiation and a control unit of a photodiode strip.

An interferometer for scribing slits on diffraction gratings and an optical scheme of the spectrometer were computed with simultaneous optimization and minimization of main aberrations in the working wavelength range of the spectrometer. The concave substrate with the evaporated photoresist was exposed in the field of a dual-beam interferometer and then developed in a special low-contrast solution to produce a surface relief. Then reflecting coatings

from $\text{Al}+\text{MgF}_2$ were deposited on the surfaces of the diffraction gratings. The gratings were tested for an operating model of a single-band spectrograph. Its external view is shown in Fig. 1. A concave holographic grating is the main unit of the optical scheme of the spectrograph. The gratings developed by us are complex diffraction units. Variable spacing and curvilinear slits are capable of reducing several times the astigmatism and coma in comparison with

conventional gratings. The diffraction grating of the spectrograph performs the functions of focusing, correcting, and dispersive units and has the flat detection field for multichannel spectrometry. The spectrograph is of the simplest design. A photodiode strip placed in the exit plane of the spectrograph to record wavelength spectra is controlled by an IBM PC. A modular design of the operating model had allowed us to realize different configurations depending on its function when we carried out our tests. To this end, the operating model was equipped with a changeable source of radiation.

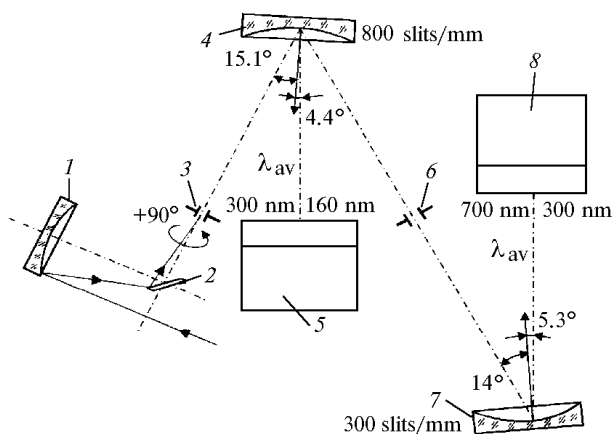


FIG. 2. Optical scheme of a two-band spectrograph comprising the concave holographic diffraction gratings 4 and 7, the slits 3 and 6, and the electron-optical image converters 5 and 8 linked to the photodiode strips. The Newton telescope comprises the principal mirror 1 and the flat mirror 2; $+90^\circ$ denotes the optical axis perpendicular to the meridional plane of the spectrograph.

Figure 2 shows the optical scheme of the two-band (160–300 nm, $\Delta\lambda = 1$ nm; 300–700 nm, $\Delta\lambda = 2$ nm) small-size (526×370×100 mm) spectrograph intended for studying and monitoring of the atmospheric state. It comprises two concave holographic gratings with radii of curvature of 22.34 cm. A light beam focused with illumination optics was transmitted through the entrance slit 112 μm in diameter and then was incident on the first grating operating in the UV range between 160–300 nm. The grating has 800 slits/mm, curvilinear slits, and variable slit spacing. Conditions of recording for the grating were chosen starting from the mutual arrangement of the spectrograph units and its overall dimensions. The light beam was incident on the grating at an angle of 15.1° . This angle is optimal for the arrangement of the spectrograph units and for minimization of aberrations. The angles of the grating in the plus first diffraction order are 7.61 and 1.17° , respectively, for wavelengths of 160 and 300 nm.

To achieve higher spectral resolution, the optical scheme of the spectrometer was computed for the case in which the light source (the entrance slit) and the detection plane were beyond the Rowland circle. In this case, optimization of aberrations in the computations (only the angle of incidence of the input beam remained constant, whereas the rest of the parameters were varied) allowed us to achieve a higher spectral resolution in the entire spectral range.

The detection plane was perpendicular to the direction of incidence of the beam whose wavelength was in the middle of the examined spectral range. The optical scheme was computed with consideration for recording of the spectrum with the plane detector – the photodiode strip. For the above-indicated spectral range we obtained two stigmatic points (at which the meridional astigmatism vanished) by way of optimization, that is, by a serial search for the parameters of optical system. Adjacent spectral points also have low meridional astigmatism, because it changes its sign at the stigmatic points. The optical scheme of the spectrometer belongs to the schemes with the flat detection field, and we have computed the aberrations exactly for this detection plane.

The output radiation from the first grating in the zeroth diffraction order that comprises about 40% of the total one was transmitted through an intermediate slit having an aperture 150 mm in diameter, and then was incident on the second grating having 300 slits/mm, which was computed for the spectral range between 300–700 nm. The angle of radiation incidence on the grating, being equal to 14° , and the plus-first order diffraction angles being equal to 8.74 and 1.83° for wavelengths of 300 and 700 nm, respectively, were chosen from the same considerations as for the first grating.

Figure 3 shows the values of sagittal and meridional astigmatism for both gratings in the detection plane. The aberrations for simple concave diffraction gratings with constant spacing of slits are also shown in Fig. 3 for comparison. The astigmatism of the grating is characterized by the spot size (along the diameter) in the detection plane on the photodiode strip. The meridional astigmatism is measured in the plane which comprises the incident and diffracted beams, and its value specifies the spectral resolution of the grating; the sagittal astigmatism is the spot size on the strip in the vertical direction and its value depends on the degree of focusing of the diffracted light beam. The latter parameter is important, because the height of the photodiodes in the strip usually lies in the range 25–500 μm .

The decrease of the aberrations through their correction allowed us to achieve high spectral resolution for small overall dimensions and large aperture ratio of the spectrograph. The aperture ratio is specified by the ratio of the relative aperture of the spectrograph and gratings and is equal to $1/3$. The diffraction efficiency of the gratings with sinusoidal

slits is $\sim 20\%$ in the visible range. It is 1.5 times greater in the UV range. The entrance slit diameter of the spectrograph is $112\ \mu\text{m}$. The reciprocal linear dispersion of the first grating is $61.5\ \text{\AA}/\text{mm}$ and of the second grating is $160\ \text{\AA}/\text{mm}$. For these values of the parameters the meridional aberration can be considered vanishing, and in fact the spectral lines can be transferred from the entrance plane to the exit one practically without astigmatism.

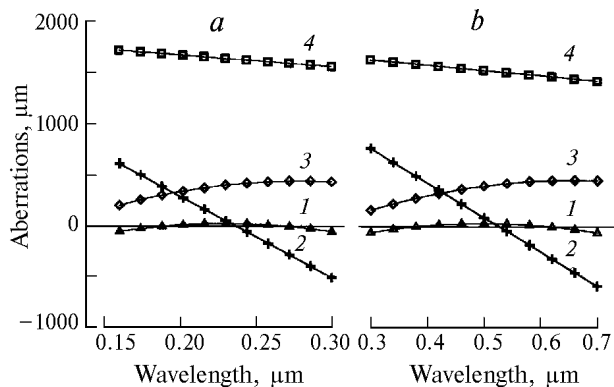


FIG. 3. Astigmatism of diffraction grating having a radius of curvature of 22.34 cm (a, b) and 800 (a) and 300 (b) slits/mm in the wavelength ranges 160–300 (a) and 300–700 nm (b). Here, curve 1 is for the meridional and curve 2 is for the sagittal astigmatism of the holographic diffraction gratings; curve 3 is for the meridional astigmatism and curve 4 is for the sagittal astigmatism of simple concave gratings.

In so doing, the spectral resolutions are 7 and $16\ \text{\AA}$ for the visible and UV ranges, respectively. The photodiode strips recorded the spectra with spectral resolution no worse than 10 and $20\ \text{\AA}$ in the above-indicated spectral ranges. This spectral resolution meets the condition $\lambda/\Delta\lambda \geq 100$, which is required for the majority of atmospheric investigations by the optical methods in accordance with the conclusions of Ref. 4. To ensure 95% accuracy of reconstruction of individual spectral lines in the visible range, five elements of linear photodetector should record $8\ \text{\AA}$ of the spectrum, whereas ten elements should record $7\ \text{\AA}$ of the spectrum in the UV range.

The flat detection field of the spectrometer makes it feasible to use multichannel systems to record the spectra, for example, the LF1024-2/2 (with 1024 elements) photodiode strips produced in our country. A device to control with the strip was developed by us. It was used for recording and storage of the spectra. A signal from the photodiode strip was amplified and fed into an analog-to-digital converter compatible with an IBM PC. The signal converted into its digital code in the edge of a synchronizing signal was stored. The spectrum was displayed on a screen. The dynamic range of the converter was 10 bits, its conversion time was $20\ \mu\text{s}$. A timer was used to choose the exposure time and to generate control signals. The exposure time was in

the range from 10 to 3000 ms depending on the signal amplitude.

Owing to the variable exposure time which can be changed 300 times and the 10-bit ADC, the spectrograph was capable of measuring signals with intensities changing $3 \cdot 10^5$ times. The threshold sensitivity of the photodiode strip (limited by noise) is $0.05\ \mu\text{J}$ at a wavelength of $0.63\ \mu\text{m}$. The noise level halves as the temperature decreases down to 5°C . To increase the sensitivity, the spectra were recorded with electron-optical image converters (EOICs) having glass fiber terminal linked to the photodiode strips.

Figure 4 shows some results of investigations of the spectral resolution and measurements of the instrumental line profiles and scattered light intensity.

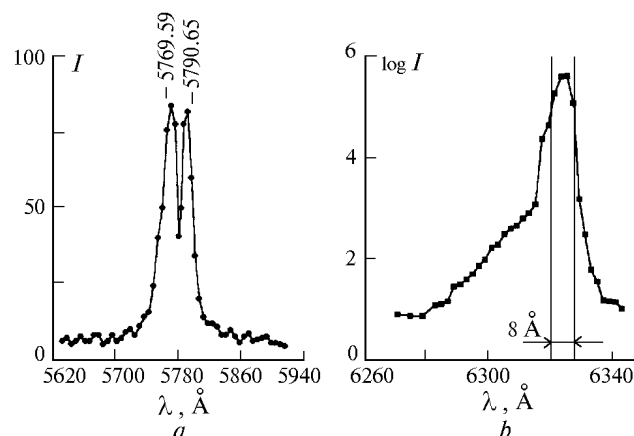


FIG. 4. Results of investigations of the resolving power of the spectrograph and the intensity of scattered light: spectrogram of the Hg doublet with $\lambda_1 = 5769.59\ \text{\AA}$ and $\lambda_2 = 5790.65\ \text{\AA}$ (a), in relative units, recorded with the photodiode strip; experimental instrumental profile of the line centered at $\lambda = 6324\ \text{\AA}$ (b).

The results of testing demonstrate that the spectrograph with photoelectric recording using the LF1024-2/2 photodiode strip resolves the spectral lines spaced at $20\ \text{\AA}$ in the wavelength range 300–700 nm and at $10\ \text{\AA}$ in the range 160–300 nm. A spectrogram of the Hg doublet with $\lambda_1 = 5769.59\ \text{\AA}$ and $\lambda_2 = 5790.65\ \text{\AA}$ is shown in Fig. 4a as an example. The doublet recorded by the photodiode strip meets the Rayleigh condition of resolution. Five elements of the strip operate within a $21\ \text{\AA}$ spectral range. This agrees well with the measurements of the instrumental line profile centered at $\lambda \sim 6324\ \text{\AA}$ (radiation emitted by a He-Ne laser) shown in Fig. 4b. The laser radiation transmitted through interface optics was incident on the entrance slit $50\ \mu\text{m}$ in diameter. The exit slit $10\ \mu\text{m}$ in diameter was placed in the exit plane.

The radiation upon exiting from the slit was recorded with a PMT having a low dark current. The

linear regime of measurements in the working range that comprised 6 orders of magnitude of the radiant intensity was provided by the application of calibrated optical filters. The expected half-linewidth determined by the entrance slit diameter and the amount of dispersion and being equal to 8 \AA agrees well with the experimental one. As seen from Fig. 4b, the scattered light intensity at a distance of 20 \AA from the edge of the entrance slit image is 4.5 orders of magnitude less than in the line center. The intensity of scattered light is an important parameter of the device for studying the spectra of the Earth's atmosphere, especially in the UV range.¹⁸ To the preceding we can add that in the case of visual study of the maximum resolution of the spectrometer with the help of a horizontal microscope, the Na doublet with $\lambda_1 = 5889 \text{ \AA}$ and $\lambda_2 = 5895 \text{ \AA}$ ($\Delta\lambda = 6 \text{ \AA}$) was easily distinguished when the entrance slit diameter was less than 50 \mu m . Our study of the spectra in the UV range with the use of the electron-optical image converter to convert the UV radiation into the visible one demonstrated that the lines spaced at $7\text{--}10 \text{ \AA}$ were well distinguished when the entrance slit diameter was 112 \mu m .

A rapid (1/3) Newtonian telescope ($\varnothing 100 \text{ mm}$) was used for illuminating optics. The field of view of the spectrometer with this telescope was $2\beta = 1.2 \text{ min}$ of arc when the entrance slit was round and had a diameter of 112 \mu m . This is supported by the results of testing of the spectrometer with the use of wide miras (test patterns).

REFERENCES

1. Yu.M. Timofeev, *Izv. Akad. Nauk SSSR, Fiz. Atmos. Okeana* **25**, No. 5, 451–472 (1989).
2. E.A. Aleksandrov, Yu.A. Izrael', I.L. Karol', and A.Kh. Khrgian, *Ozone Shield of the Earth and Its Variations* (Gidrometeoizdat, St. Petersburg, 1992), 288 pp.
3. G.M. Krekov and S.G. Zvenigorodskii, *Optical Model of the Middle Atmosphere* (Nauka, Novosibirsk, 1990), 278 pp.
4. V.A. Krasnopol'skii, *Physics of the Glow in the Atmospheres of Planets and Comets* (Nauka, Moscow, 1987), 304 pp.
5. B. Stark and L. Martini, *Absorptionsspektroskopische Messungen auf Raketen und Satelliten für Bestimmung atmosphärischer Gaskonstituenten* (Akademie-Verlag, Berlin, 1987), 114 pp.
6. A. Schnapf, ed., *Progress in Astronautics and Aeronautics* **97**, 830 (1985).
7. K.Ya. Kondratyev and O.M. Pokrovsky, *Geophysica Inter.* **29**, No. 1, 29–34 (1990).
8. D.F. Khit and D.B. Khini, in: *Space Optics* (Mashinostroenie, Moscow, 1980) pp. 226–237.
9. A.I. Lebedinskii, A.I. Krasnopol'skii, A.P. Kuznetsov, and V.A. Iozenas, in: *Space Research* (Nauka, Moscow, 1965), p. 77.
10. D.A. Andrienko, V.I. Barysheva, V.N. Vashchenko, et al., *Issled. Zemli iz Kosmosa*, No. 1, 67–73 (1990).
11. A.L. Broadfoot, B.R. Sandel, D.E. Shemansky, et al., *Space Sci. Rev.* **21**, 183 (1977).
12. M.R. Torr and R.C. Vitz, *Appl. Opt.* **21**, No. 17, 3080–3090 (1982).
13. J.B. Pranke, A.B. Chistensen, F.A. Morse, et al., *Appl. Opt.* **21**, No. 21, 3941–3952 (1982).
14. D.P. Heath, F.J. Krueger, H.A. Roeder, and B.D. Henderson, *Opt. Eng.* **14**, No. 4, 323–331 (1975).
15. J.B. Pearce, K.A. Gause, E.F. Mackey, et al., *Appl. Opt.* **10**, 805 (1971).
16. V.A. Krasnopol'skii, A.A. Krys'ko, V.N. Rogachev, and V.A. Parshev, *Kosmich. Issled.* **14**, 789 (1976).
17. G.P. Reddy and M. Singh, *J. Optics (Paris)* **19**, No. 2, 77–82 (1988).
18. A.A. Cheremisin, L.V. Granitskii, V.M. Myasnikov, et al., *Atmos. Oceanic Opt.* **10**, No. 12, 885–890 (1997).